Asian Journal of Chemistry; Vol. 38, No. 4 (2026), 1045-1051
ASIAN JOURNAL OF CHEMISTRY
https://doi.org/10.14233/ajchem.2026.35419

Synthesis, Crystal Structure, Spectroscopic and Computational Studies of a New Organic Crystal: Quinoxaline: 3,5-Dichloro-2-hydroxybenzoic Acid

C. KOHILA[1], G. DINESH KUMAR[1,*], G. KAVITHA[1] and S. JYOTHI[2]

[1]Department of Chemistry, Gobi Arts & Science College, Gobichettipalayam-638453, India
[2]Department of Chemistry, Kumaraguru College of Technology, Coimbatore-641006, India

*Corresponding author: E-mail: dineshchem@gascgobi.ac.in

Received: 8 December 2025 *Accepted*: 5 March 2026 *Published online*: 8 April 2026 AJC-22327

A new molecular cocrystal of quinoxaline with 3,5-dichloro-2-hydroxybenzoic acid (QODCS) was synthesised by slow evaporation technique and its structural, spectral, thermal and nonlinear optical properties were studied. Single crystal X-ray diffraction revealed that the crystal belongs to the triclinic system with $P\bar{1}$ space group and is stabilised by hydrogen bonding and π···π interactions. FT-IR and UV–Vis analyses confirmed the formation of the cocrystal and the presence of conjugated systems. Thermal analysis showed that the material is stable up to 286 ºC with single-stage decomposition. Hirshfeld surface and NBO analyses indicated strong intermolecular interactions and effective charge transfer within the system. Theoretical UV studies supported π-electron delocalisation through HOMO–LUMO transitions. The crystal exhibited enhanced dipole moment and significant hyperpolarizability values, indicating strong nonlinear optical behaviour.

Keywords: Slow evaporation, QODCS, Thermal analysis, Hirshfeld surface, Optical properties.

INTRODUCTION

Cocrystals are solids that are neutral crystalline single phase materials composed of two or more different molecular and/or ionic compounds generally in a stoichiometric ratio which are neither solvates nor simple salts [1]. In recent era, the researchers pay more attention on organic crystals than inorganic due to their high flexibility, high degree of delocalisation of π-electrons, high non-linear response, *etc.* Also, organic crystals are found to have potential applications in the field of pharmaceutical, optical communications, optical computing, optical switches, frequency doubling and materials science, *etc.* [2-4]. The crystal engineering is noteworthy in constructing supramolecular structures with desired physico-chemical properties.

Hydrogen bonding plays a significant role in crystal engineering among various non-covalent interactions present in organic molecules [5]. The crystals are usually formed between donor and acceptor molecules, they tend to form a molecular complex and they are treated as a resonance hybrid of two structures. One of them is considered to be no bond structure [DA] in which the molecular components are bound by weak van der Waals interactions. Another one, in which the donor and acceptor species are held together by strong ionic bond [D^+A^-] [6]. As carboxylic acids have good supramolecular properties and strong hydrogen bonding ability, they are often chosen as a donor in crystal engineering [7]. Similarly, the organic compounds with hetero atoms are frequently employed as an acceptor. The molecular complexes formed due to electron donor-acceptor were seemed to be less stable as a result of weak electrostatic interactions. Whereas, the molecular complexes formed because of proton transfer are found to be more stable due to strong ionic interactions [8].

The quinoxaline scaffold holds significant importance in various fields of medicinal and material chemistry. It exhibits a wide range of applications, including antibacterial [9], antitubercular [10] and antimalarial activities, as well as in the development of electroluminescent materials, molecular probes, fluorescent materials, organic sensitizers for solar cells and polymeric optoelectronic materials. Moreover, quinoxaline also used for crop protection in agro-industries, as a major component of insecticides [11], herbicides [12] and fungicides [13]. Besides their medicinal and crop protection applications [14], they are also employed as organic semiconductors and corrosion inhibitors for metals [15,16]. However, comprehensive investigations into their crystal growth behaviour, optimi-

sation of growth parameters and mechanistic aspects are still limited. The majority of previous studies focus mainly on the synthetic methodologies and functional applications, with comparatively little emphasis on obtaining high-quality single crystals or controlling morphology, defect formation and crystal engineering parameters. Furthermore, when compared to other heterocyclic systems, quinoxaline-based cocrystals and supramolecular assemblies remain insufficiently explored, particularly for tailoring optical and nonlinear optical responses. Although theoretical studies predict promising electronic and optical properties, experimental validation through single-crystal analyses is relatively scarce, leading to a gap between computational predictions and experimental evidence.

Similarly, hydroxybenzoic acid have been highly noticed due to their significant *in vitro* antimicrobial and antifungal activities [17]. Based on these aspects, in present work, quinoxaline and 3,5-dichloro-2-hydroxybenzoic acid were utlised for the crystal growth. The grown crystals are subjected to various characterisation techniques.

EXPERIMENTAL

Analytical grade quinoxaline (QO) and 3,5-dichloro-2-hydroxybenzoic acid (DCS) was taken in a definite stoichiometric ratio, 1:1 by weight. For the crystallisation process, a solvent assisted grinding method was adapted. A few drops of methanol were added in the stoichiometric mixture of both reactants while grinding with a help of a mortar and a pestle for about 15 to 20 min. The finely ground homogeneous mixture was dissolved in methanol and kept undisturbed in a perforated beaker. High-quality quinoxaline:3,5-dichloro-2-hydroxybenzoic acid (QODCS) crystals were successfully grown (**Scheme-I**) using the slow solvent evaporation technique. The cocrystal was obtained in good yield from the stoichiometric amounts of the components under optimized conditions. The obtained crystals were further subjected to various physico-chemical characterisations.

RESULTS AND DISCUSSION

Single crystal XRD studies: The crystal structure of the synthesised QODCS was confirmed using single crystal X-ray diffraction analysis (ORTEP view is given in Fig. 1). The crystallographic data of QODCS is given in Table-1, which

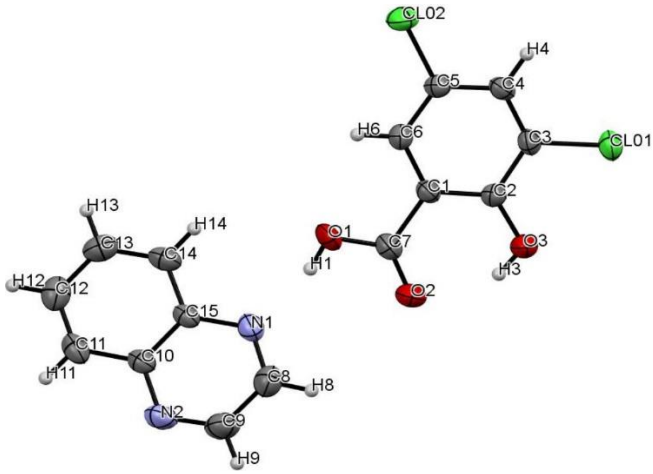

Fig. 1. ORTEP of QODCS showing the atom labelling scheme at 30% probability level

TABLE-1
CRYSTALLOGRAPHIC DATA FOR QODCS

Chemical formula	$C_{15}H_{10}Cl_2N_2O_3$
M_r	337.15
Crystal system, space group	Triclinic, $P\bar{1}$
Temperature (K)	298
a, b, c (Å)	3.8552 (9), 13.039 (3), 14.563 (4)
α, β, γ (º)	80.903 (6), 83.121 (6), 86.496 (6)
V (Å^3)	717.0 (3)
Z	2
Radiation type	Mo$K\alpha$
m (mm^{-1})	0.47
Crystal size (mm)	0.20 × 0.20 × 0.20
Diffractometer	Rigaku mercury 375R (2 × 2 bin mode)
Absorption correction	Multi-scan Jacobson, R. (1998) Private communication
T_{min}, T_{max}	0.663, 1.000
No. of measured, independent and observed [I > 2s(I)] reflections	7153, 3230, 2483
R_{int}	0.029
R[F^2 > 2s(F^2)], wR(F^2), S	0.049, 0.143, 1.18
No. of reflections	3230
No. of parameters	201
H-atom treatment	H-atom parameters constrained
$D\rho_{max}$, $D\rho_{min}$ (e Å^{-3})	0.32, -0.38

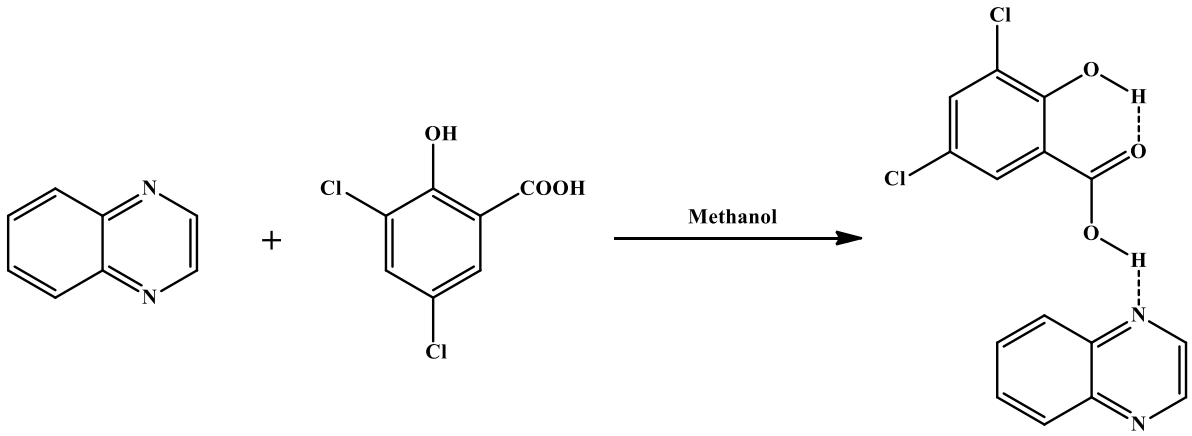

Scheme-I: Synthesis of quinoxaline:3,5-dichloro-2-hydroxybenzoic acid (QODCS) co-crystal

shows the cocrystals crystallises in a triclinic system with $P\bar{1}$ space group. Various inter and intramolecular hydrogen bonding interactions are shown in Table-2. In the asymmetric unit, the QO and DCS molecule lie in a twisted plan with a dihedral angle of 27.09º to each other favours various types of interactions like π···π, C–Cl···π, O–H···N, O–H···O, C–H···N and C–H···O interactions which stabilize the molecule. The molecule exhibits abundant π···π stacking interactions that extend along the *a*-axis (symmetry operations: -1+X,Y,Z; 1+X,Y,Z; 1-X,1-Y,1-Z; -1+X,Y,Z; 1+X,Y,Z), contributing significantly to the stabilisation of the crystal packing. It is interesting to observe that QODCS has C–Cl···π interactions as observed in the literature for chlorine derivatives. On extending *c*-axis, QODCS has face to face π···π and C–Cl···π stacking interactions. In addition to their stacking interactions, the molecule is linked with numerous intra and inter molecular hydrogen bonding interactions. Carboxylic group of DCS moiety is known to form ring graph set format of hydrogen bonding interactions. With no surprise, the carboxylic O–H forms O1-H1···N1 interactions with neighboring pyrazinyl nitrogen and pyrazinyl C8-H8 forms C8-H8···O3 interactions with neighbouring DCS moiety leads to R_2^2 (12) graph set. The DCS moiety also connected through intermolecular O3–H3···O2 hydrogen bonding interactions which arises from hydroxyl group of one of the molecules with the carboxylic C=O of another DCS moiety. This type of interactions forms various graph sets like R_3^3 (9), R_2^2 (12), *etc.* which is clearly seen while extending the molecule at *a*-axis. Interestingly, QODCS also has rich chlorine and Cl···H interactions. The hydroxyl group in the second position for DCS moiety favours intramolecular O3-H3···O2 hydrogen bonding interactions. The hydrogen attached to the carbon in the sixth position bring forth C6-H6···O1 intramolecular interactions with the neighbouring carboxylic O–H. Thus, the QODCS molecule is stabilised with the numerous and extend of different molecular interactions [18].

Electronic spectral features: Electronic transition spectrum of QODCS dispersed into methanol solvent was observed, which is apparent in Fig. 2. The spectrum shows an identifiable absorption band at 247 nm, that is associated to π-π* absorption of the aromatic ring and 312 nm, which is associated to n-π* bands of the QODCS compound [19].

FT-IR spectral studies: The FT-IR spectrum is displayed in Fig. 3 and the various functional groups present in the crystal QODCS is verified. Spectrum indicates that the O–H stretching vibration is responsible for the band at 3040 cm^{-1}. The aromatic C=C stretching vibrations are represented by the absorption bands at 1497 and 1579 cm^{-1} correspondingly.

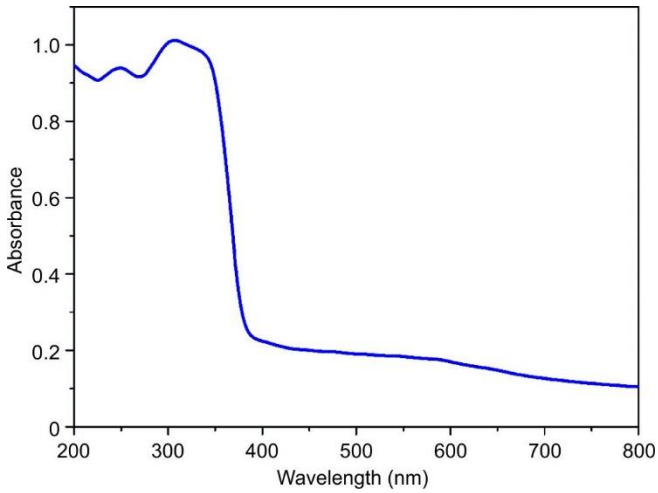

Fig. 2. UV-Visible absorption spectrum of QODCS

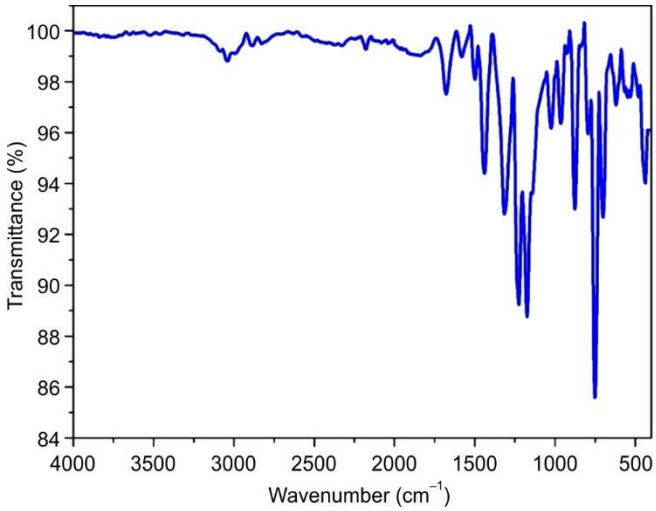

Fig. 3. FT-IR spectrum of QODCS

The C=O stretching band [20] of the DCS moiety is observed at 1680 cm^{-1} and its slight shift relative to the parent acid indicates participation in hydrogen-bond interactions with the quinoxaline nitrogen atoms. Similarly, the DCS moiety's COO stretching vibration at 1438 cm^{-1} reflects changes in the electronic environment upon cocrystallisation. The absorption peak at 748 cm^{-1} is attributed to the aromatic C–H out-of-plane bending vibration. At 694 cm^{-1}, the C–Cl stretching vibration is observed [21]. The C–N stretching vibration at 874 cm^{-1} and the NCC bending mode near 969 cm^{-1} exhibit slight deviations compared to parent quinoxaline, indicating its interaction with the acid moiety.

TABLE-2
NON-COVALENT AND HYDROGEN BOND INTERACTIONS DATA IN QODCS

Donor···Acceptor	D–H (Å)	H···A (Å)	D···A (Å)	D–(H)···A (º)	Symmetry
O1–H1···N1	0.82	1.83	2.625(3)	165	–
O3–H3···O2	0.82	1.93	2.638(3)	145	–
O3–H3···O2	0.82	2.55	3.120(3)	128'	1-x,1-y,2-z
C4–H4···N2	0.93	2.60	3.528(4)	175	1+x,1+y,z
C6–H6···O1	0.93	2.38	2.709(3)	100	–
C3–Cl01···π	–	–	3.7388(17)	67.53(9)	1+x,y,z

Thermal studies: The thermal characteristics of the QODCS crystal were investigated using thermogravimetric and differential thermal investigations. The TG curve (Fig. 4) shows that the crystalline material broke down right away after melting and that there was no discernible weight loss up to 286 ºC. Decomposition occurs in a single step at a high temperature, yielding volatile gaseous products such as NH_3, CO_2, NO_2 and HCl. One possible residue that is left over after the breakdown is a stable carbon molecule. The TG curve and the DTA curve both display the same changes. The material's melting point is indicated by the steep endothermic dip at 286 ºC [22].

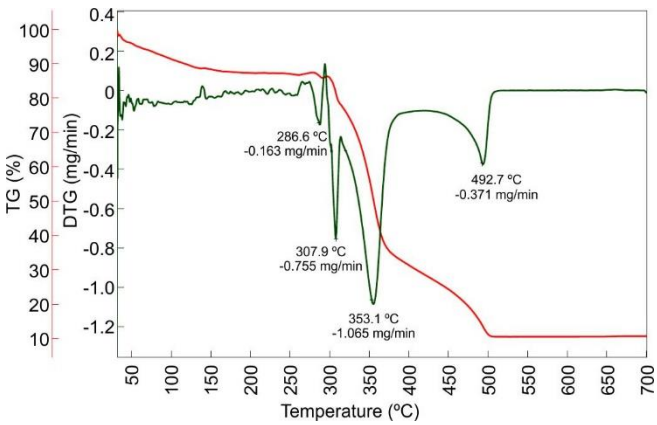

Fig. 4. Thermogram curves of QODCS

Hirshfeld surface studies: The Hirshfeld surface analysis was carried out for QODCS by using the .cif file (Fig. 5). The red spots are identified over phenylic hydrogen of pyrazinyl moieties as well as hydroxyl hydrogen of salicylic moiety in the d_i surfaces for QODCS. In d_e surfaces, strong red spots appear on pyrazinyl nitrogen as well as the chlorine atom of salicylic acid. Even though there are numerous hydrogen bonding interactions observed with the help of SCXRD, the hydrogen bonds involved with pyrazinyl nitrogen and carboxylic oxygens as well as hydroxyl group of salicylic acid moieties are dominant in QODCS. The fact is supported by the fingerprint plots in which O···H/H···O and N···H/H···N contacts contribute 15.3 and 6.1%, respectively. This is due to the inter and intramolecular hydrogen bonding interactions as shown in Table-2. It is observed that QODCS enriched with different stacking interactions such as π···π, C3-ClO1···π, *etc.* which were verified from C···C and Cl···C/C···Cl contacts contributing 9.9 and 3.1%, respectively. Other major contacts observed are Cl···Cl, C···H/H···C and H···H contributes 3.8, 12.0 and 21.4 %, respectively to the total Hirshfeld surfaces. Notably the hydrogen bonding interaction involving chlorine (Cl···H/H···Cl contacts) is proved by the contribution of 21.3% to the total Hirshfeld surfaces. This contacts also appears as a pair of spikes in the 2D fingerprint plots (Fig. 6) along with another couple of spikes which belongs to the O···H/H···O and N···H/H···N contacts. The curvedness and shape index indices support the contribution of stacking interactions involved in the stabilisation of QODCS molecule.

NBO analysis: NBO analysis has been carried out for QODCS. It is found from the data that the molecule exhibits conjugative and hyper conjugative interactions. The major conjugative interactions have been arising due to the transfer of LP(1) C19→π* N18-C31, LP(1) C19→ π* C21-C25, π N18-C31→π* N17-C29, π C21-C25→π* C23-C27, π C23-

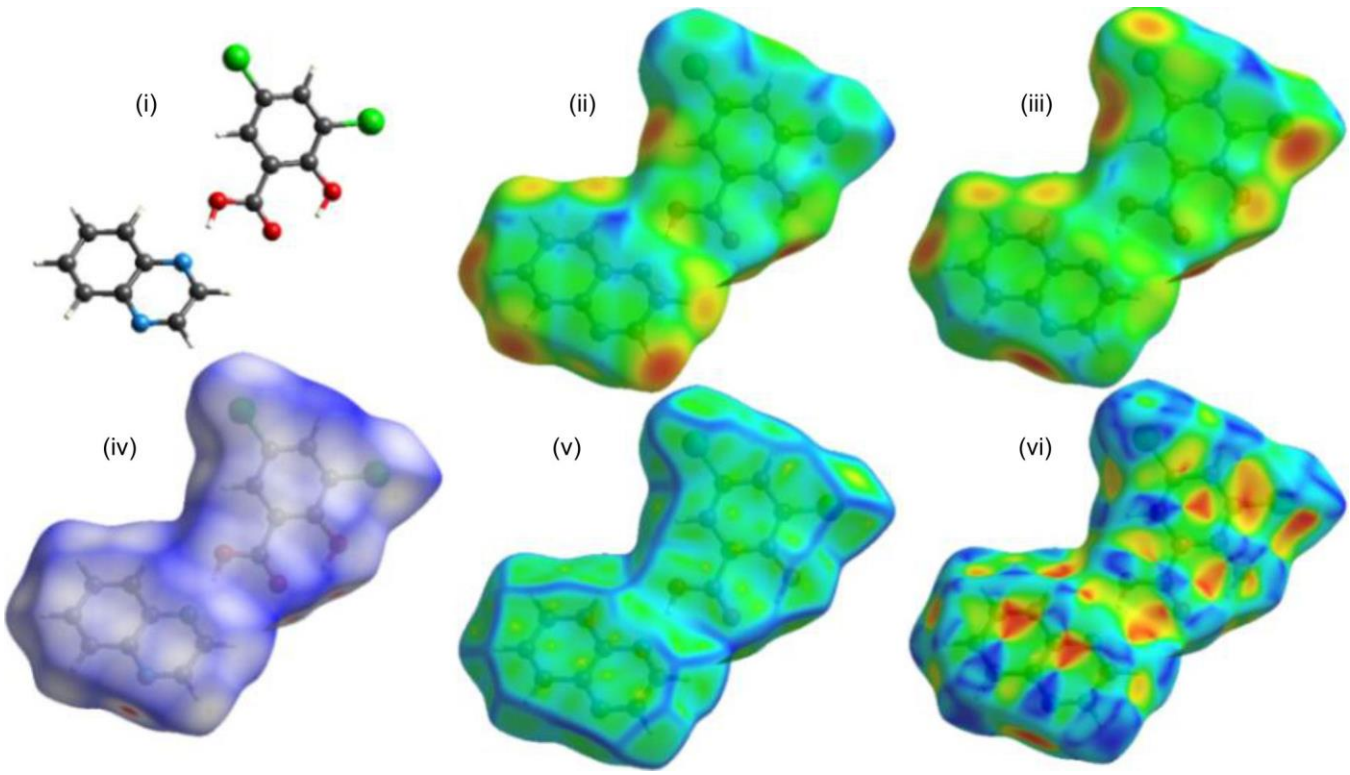

Fig. 5. Molecular structure of QODCS (i) Hirshfeld surfaces mapped on (ii) d_i, (iii) d_e, (iv) d_{norm}, (v) shape index and (vi) curvedness

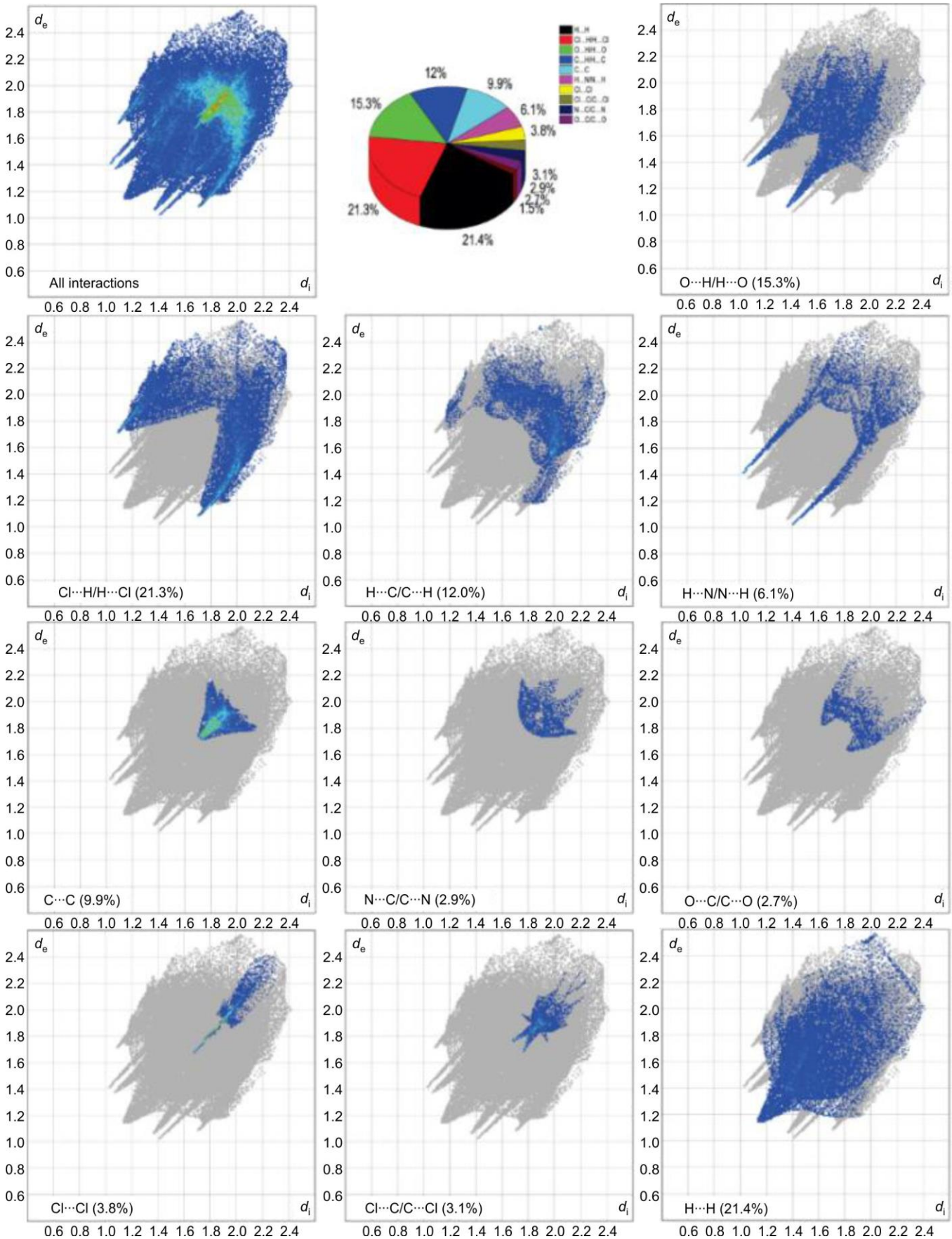

Fig. 6. Fingerprint plot for QODCS

C27→π* C21-C25, π N17-C29→π* N18-C31 with the larger stabilisation of 60.11, 48.56, 17.83, 17.73, 16.73 and 13.63 kcal/mol. It is also interesting to observed that there are inter and intramolecular conjugative interactions arises with the transfer of LP(2) O6→π*O5–C16, LP (2) O3→π*C14–C15, πC14–C15→π*C8–C11, πC18–C11→ π*C10–C12, πC10–C12→π*C14-C15, πC14–C15→π*C10-C12, πC10–C12→ π*C8-C11, πC8-C11→π*C14-C15 with stabilisation energies 59.71, 39.65, 26.09, 25.45, 23.41, 21.83, 16.04, 15.13 and 14.52, respectively. The presence of electronegative chlorine atoms in the phenylic moiety arises a couple of interactions, *viz.* LP(3) Cl1→π* C10–C12 and LP(3) Cl2→ –π*C8-C11 with stabilisation energies, 12.38 and 11.6, respectively. It is noted that there are numerous hyperconjugative interactions arises due to the molecular interactions.

Theoretical UV analysis: The theoretical UV-spectra has been calculated for QODCS (Fig. 7). A major peak observed at around 337 nm with an oscillator strength of 0.0006 is due to the HOMO→LUMO transitions. From the CHELPG atomic charges analysis, it was found that the potential of 3,5-dichloro salicylic acid moiety and quinoxaline are -0.214232e and +0.214232e, respectively reveals that the former is an electron acceptor and the latter is an electron donor. The high oscillator strength are observed at the wavelength of 305 and 282 nm for the transitions HOMO→LUMO+1 (92%), HOMO-4→LUMO+3 (4%), HOMO-1→LUMO (2%) and HOMO-3 →LUMO (78%), HOMO-1→LUMO+2 (20%), respectively. These transitions are due to the π···π interactions found in the QODCS molecule.

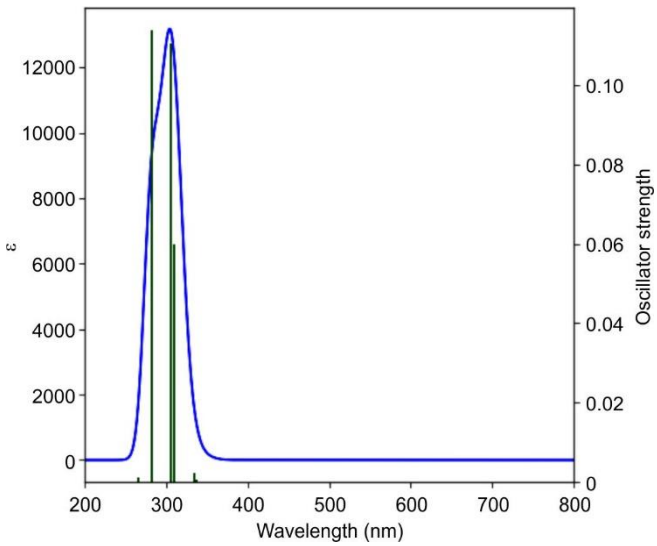

Fig. 7. Theoretical UV spectrum of QODCS calculated at B3LYP/6-311G(d,p) level

Microscopic optical properties: The strong optical response of QODCS at ω = 0.0428 a.u., summarised in Table-3, can be attributed to the significant intermolecular interactions within the crystal lattice. The dipole moment of the crystal is 6.2899 Debye, which was strongly influenced by μ_z component is higher than that of many conventional organic NLO materials such as urea and simple π-conjugated systems indicating strong molecular asymmetry and efficient intramolecular charge transfer, a key requirement for enhanced non-linear optical response [23]. The static and frequency dependent isotropic hyperpolarizability for QODCS are found to be 31.551 and 32.092 (× 10^{-24} esu), respectively. The DC pockels effect and frequency dependent first hyperpolarizability are found to have increase of 13% and 49.8%, respectively with respect to the static hyperpolarizability of 2.262 × 10^{-30} esu. The trend has been extended on second hyperpolarizabilities as the Kerr effect and frequency dependent second hyperpolarizabilities are increased by 9.3% and 39.2 %, respectively over the static second hyperpolarizability of 14.144 × 10^{-36} esu. It is significantly higher than those of many simple organic crystals and comparable to advanced donor–acceptor substituted systems and π-delocalised frameworks reported [24,25]. These enhanced dipole moment, first-order (β) and second-order (γ) hyperpolarizability values, confirming its potential as a promising candidate for second harmonic generation and third-order nonlinear optical applications.

TABLE-3
MICROSCOPIC OPTICAL PARAMETERS DATA FOR QODCS

Property	Components	Values
Dipole moment (Debye)	μ_{tot}	6.2899
Polarizability	α_{xx}	13.861
α (0;0)	α_{yx}	6.701
(× 10^{-24} esu)	α_{yy}	37.318
	α_{zx}	0.484
	α_{zy}	1.869
	α_{zz}	43.473
	<α>	31.551
	Δα	29.638
Polarizability	α_{xx}	13.942
α (-ω,ω)	α_{yx}	6.855
(× 10^{-24} esu)	α_{yy}	37.938
ω =0.0428 a.u.	α_{zx}	0.507
	α_{zy}	1.957
	α_{zz}	44.397
	<α>	32.092
	Δα	30.426
$\beta_{\|}$ (0;0,0) (× 10^{-30} esu)	Static	2.262
$\beta_{\|}$ (-ω;ω,0) (× 10^{-30} esu)	ω = 0.0428 a.u.	2.556
$\beta_{\|}$ (-2ω; ω,ω) (× 10^{-30} esu)	ω = 0.0428 a.u.	3.389
γ(0; 0,0,0)	γ_{xxxx}	0.466
× 10^{-36} esu	γ_{yyyy}	11.636
	γ_{zzzz}	36.559
	γ_{xxyy}	1.142
	γ_{xxzz}	1.180
	γ_{yyzz}	8.693
	$\gamma_{\|}$	14.144
γ(-ω;ω,0,0)	γ_{xxxx}	0.482
ω = 0.0428a.u	γ_{yyyy}	12.380
× 10^{-36} esu	γ_{zzzz}	40.430
	$\gamma_{\|}$	15.461
γ(-2ω;ω,0,0)	γ_{xxxx}	0.519
ω =0.0428a.u	γ_{yyyy}	14.148
× 10^{-36} esu	γ_{zzzz}	54.055
	$\gamma_{\|}$	19.690

Conclusion

A new crystal with interesting microscopic properties has been explored in this study with the help of both experi-

mental and theoretical analysis. SCXRD experimentally confirms that QODCS is stabilised by an extensive network of hydrogen bonding, chlorine interactions and π–π stacking interactions. The presence of various functional groups in the QODCS compound has been confirmed experimentally by FT-IR spectroscopic study. The thermal stability of the co-crystal was determined by TG/DTA studies and it can be used in high temperature applications. The contribution of each interaction has been proved from the 2D fingerprints and Hirshfeld surfaces. In contrast, the electronic structure and charge transfer characteristics of QODCS are derived from theoretical investigations. In QODCS, significant charge transfer is observed due to extensive intermolecular interactions, as evidenced by NBO analysis and theoretical UV spectral studies. This charge transfer influences the microscopic optical properties under the applied frequency. The QODCS crystal exhibits more than 20% enhancement in hyperpolarizability at an applied frequency of ω = 0.0428 a.u. The experimental molecular geometry obtained from XRD data agrees well with the optimized structure calculated using the B3LYP method. These findings suggest that QODCS is a promising candidate for further studies aimed at exploring its advanced optical and nonlinear optical applications.

ACKNOWLEDGEMENTS

The authors acknowledge the Common Instrumentation Centre at Gobi Arts & Science College, Gobichettipalayam, which is supported by the DST-FIST Scheme.

CONFLICT OF INTEREST

The authors declare that there is no conflict of interests regarding the publication of this article.

DECLARATION OF AI-ASSISTED TECHNOLOGIES

During the preparation of this manuscript, the authors used an AI-assisted tool(s) to improve the language. The authors reviewed and edited the content and take full responsibility for the published work.

REFERENCES

1. M. Karimi-Jafari, L. Padrela, G.M. Walker and D.M. Croker, *Cryst. Growth Des.*, **18**, 6370 (2018); https://doi.org/10.1021/acs.cgd.8b00933
2. S. Anandhi, M. Rajalakshmi, T.S. Shyju and R. Gopalakrishnan, *J. Cryst. Growth*, **318**, 774 (2011); https://doi.org/10.1016/j.jcrysgro.2010.10.113
3. T.S. Kolev, I.V. Kityk, J. Ebothe and B. Sahraoui, *Chem. Phys. Lett.*, **443**, 309 (2007); https://doi.org/10.1016/j.cplett.2007.06.051
4. K. Singaravelan, A. Chandramohan, S. Madhankumar, M.V. Enoch and G. Vinitha, *J. Mol. Struct.*, **1194**, 57 (2019); https://doi.org/10.1016/j.molstruc.2019.05.028
5. M. Faizan, H.N.R. Vitor and S. Ahmad, *J. Mol. Struct.*, **1198**, 126894 (2019); https://doi.org/10.1016/j.molstruc.2019.126894
6. E. Selvakumar, G.A. Babu, P. Ramasamy, Rajnikant, V. Murugesan and A. Chandramohan, *Spectrochim. Acta A Mol. Biomol. Spectrosc.*, **117**, 259 (2014); https://doi.org/10.1016/j.saa.2013.07.097
7. S. Jin, X.H. Lu, D. Wang and W. Chen, *J. Mol. Struct.*, **1010**, 17 (2012); https://doi.org/10.1016/j.molstruc.2011.11.004
8. U. Neupane, M. Singh, P. Pandey and R.N. Rai, *J. Mol. Struct.*, **1195**, 131 (2019); https://doi.org/10.1016/j.molstruc.2019.05.026
9. V. Murugesan, M. Saravanabhavan and M. Sekar, *J. Photochem. Photobiol. B*, **140**, 20 (2014); https://doi.org/10.1016/j.jphotobiol.2014.07.003
10. S.K. Suthar, N.S. Chundawat, G.P. Singh, J.M. Padron and Y.K. Jhala, *Eur. J. Med. Chem. Rep.*, **5**, 100040 (2022); https://doi.org/10.1016/j.ejmcr.2022.100040
11. M.A. Alanazi, W.A.A. Arafa, I.O. Althobaiti, H.A. Altaleb, R.B. Bakr and N.A.A. Elkanzi, *ACS Omega*, **7**, 27674 (2022); https://doi.org/10.1021/acsomega.2c03332
12. P.A. Padvi, G.H. Mahale, D.E. Pawar, C.S. Falak and A.V. Kendre, *World J. Pharm. Res.*, **4**, 1892 (2015).
13. P. Teng, Y. Li, R. Fang, Y. Zhu, P. Dai and W. Zhang, *Molecules*, **29**, 2501 (2024); https://doi.org/10.3390/molecules29112501
14. G. Yashwantrao and S. Saha, *Org. Chem. Front.*, **8**, 2820 (2021); https://doi.org/10.1039/D0QO01575J
15. H. Kim, M.R. Reddy, S.S. Hong, C. Kim and S.Y. Seo, *J. Nanosci. Nanotechnol.*, **17**, 5530 (2017); https://doi.org/10.1166/jnn.2017.13841
16. J.D.S. Pereira, J.M. Neri, D.P. Emerenciano, G.R.S. de Freitas, M.B.M.C. Felipe, M.A.F. de Souza, F.G. Menezes and M.A.M. Maciel, *Quim. Nova*, **41**, 243 (2017).
17. G. Paraskevopoulos, S. Monteiro, R. Vosátka, M. Krátký, L. Navrátilová, F. Trejtnar, J. Stolaříková and J. Vinšova, *Bioorg. Med. Chem.*, **25**, 1524 (2017); https://doi.org/10.1016/j.bmc.2017.01.016
18. M. Khan, V. Enkelmann and G. Brunklaus, *Cryst. Growth Des.*, **9**, 2354 (2009); https://doi.org/10.1021/cg801249b
19. V. Murugesan, M. Saravanabhavan, A. Chandramohan, G. Raja and M. Sekar, *J. Photochem. Photobiol. B*, **151**, 248 (2015); https://doi.org/10.1016/j.jphotobiol.2015.08.011
20. Q. Fu, Y. Han, Y. Xie, N. Gong and F. Guo, *J. Mol. Struct.*, **1168**, 145 (2018); https://doi.org/10.1016/j.molstruc.2018.04.100
21. D.K. Shajan, N. Pandey, A. Ghosh, H.K. Chanduluru and P. Sanphui, *Cryst. Growth Des.*, **23**, 5289 (2023); https://doi.org/10.1021/acs.cgd.3c00485
22. A. Santha, V. Kannan, S. Ganesamoorthy and S. Brahadeeswaran, *J. Mol. Struct.*, **1302**, 137513 (2024); https://doi.org/10.1016/j.molstruc.2024.137513
23. D.S. Chemla and J. Zyss, Nonlinear Optical Properties of Organic Molecules and Crystals, Academic Press, vols. 1 & 2 (1987).
24. B. Champagne, E.A. Perpète, D. Jacquemin, S.J.A. van Gisbergen, E.-J. Baerends, C. Soubra-Ghaoui, K.A. Robins and B. Kirtman, *J. Phys. Chem. A*, **104**, 4755 (2000); https://doi.org/10.1021/jp993839d
25. M.G. Kuzyk, *Phys. Rev. Lett.*, **85**, 1218 (2000); https://doi.org/10.1103/PhysRevLett.85.1218